Laser Pulse Control of High-Conversion Free Radical Polymerization

Jaeup U. Kim

Department of Physics, Columbia University, New York, New York 10027

Ben O'Shaughnessy*

Department of Chemical Engineering, Columbia University, 500 West 120th Street, New York, New York 10027

Received May 11, 2003; Revised Manuscript Received November 3, 2003

ABSTRACT: This paper explores the possibility of controlling molecular weight distributions (MWDs) produced by linear free radical polymerization (FRP). We theoretically study pulsed laser free radical polymerization in the presence of a preprepared inert polymer matrix whose chains are longer than the entanglement threshold N_e. Under such conditions living chain termination is dominated by entanglements, and earlier theory for continuously initiated steady-state FRP predicts most termination events involve one long (entangled) and one short (unentangled) chain. When initiation is pulsed, we find three time scales are critical in determining the dead molecular weight distribution: T, the time between pulses; τ_{short}, the time for a living chain to grow from birth to length N_e; and τ_{living}, the mean living chain lifetime. If the condition $\tau_{short} \ll T \ll \tau_{living}$ is satisfied, we find the dead MWD is multimodal and entirely different than the broad steady-state MWD. The MWD peaks have width $\approx N_e$ and decay as $\sim 1/(N - N_i)^{3/2}$ far from the peak centered at N_i. The envelope of the peaks is essentially the steady-state MWD. We show that even when the background polymer matrix follows a broad MWD, pulsing still produces a multimodal product provided the mean background chain length exceeds N_e and certain other conditions are satisfied. Hence, an alternative procedure is to generate the background by standard steady-state FRP carried to high conversion. Physically, the effects derive from short−long domination. Each pulse injects fresh short living chains with which already-present long living chains terminate readily, producing dead chains. But a time τ_{short} later these new macroradicals have grown long and entangled, so termination and dead chain production are then effectively switched off until the next pulse arrives.

I. Introduction

Free radical polymerization (FRP) is used to synthesize vast quantities of polymeric material including homopolymers, copolymers, and other polymers with complex architectures.[1−8] The great advantages of the method are its relative operational simplicity and great robustness. One of the principal drawbacks is the broad and rather uncontrolled molecular weight distributions (MWDs) produced. This paper is a theoretical exploration of the possibility of generating well-characterized multimodal MWDs by laser pulse initiation of FRP in a concentrated polymer solution matrix (see Figure 1).

Our basic motivation is to predict what would happen in a careful and controlled "high conversion" laser pulse experiment which has the potential to expose fundamental FRP mechanisms emerging from previous theoretical analysis.[9,10] These mechanisms remain largely untested experimentally. A second motivation is to investigate the possibility that these ideas may lay the groundwork for new techniques which can steer FRP to generate controlled and more useful MWDs.

The idea is to initiate FRP with laser pulses in a background matrix of preprepared monodisperse polymer with chain length N_{matrix} plus unpolymerized monomer solvent (Figure 2). Here the chain length $N_{matrix} > N_e(\phi)$, where N_e is the entanglement threshold at polymer concentration ϕ. When photoinitiation commences in this environment, the living chains will be entangled in the long background chains and exhibit a behavior that is fundamentally different from the behavior in a dilute background ("low conversion").

The theory we develop below assumes the background is such that long enough living chains will be entangled. The simplest and most clear-cut way to achieve this is with a well-characterized and monodisperse background. However, even if the background is broadly distributed, entanglement of living chains will still result provided the mean background chain length is large enough. Hence, a related (and more simply executed) procedure entails powering FRP by continuous (nonpulsed) initiation from zero conversion through to a high conversion equal to the concentration of the polymer matrix in the present envisaged experiment. At this point pulsing would commence. Now in this second type of experiment the background will be polydisperse and complex. However, provided the mean chain length of this background is long enough (specifically, greater than N_e), then we expect the dead MWD contribution from the last pulsing episode will be essentially the same as what would have resulted with a monodisperse background. This is discussed in some detail in section V.

The zero conversion version of the experiment we consider is of course the well-established pulsed laser polymerization (PLP) method[11−17] used primarily to infer chain propagation constants. As will be shown, the origin of the effects we discuss in this paper is entanglement, which occurs only at high conversion. We stress the experiment we analyze here is not a zero conversion PLP experiment continued to high conversion. This point is discussed further at the end of this section.

* To whom correspondence should be addressed: e-mail bo8@columbia.edu.

10.1021/ma034607m CCC: $27.50
Published on Web 01/20/2004

Our predictions for this monodisperse matrix experiment include above all a multimodal dead MWD (see Figure 1c) and are closely related to the predictions of ref 9 for high-conversion steady-state FRP. In those works, a crucial role was played by first principles polymer physics theories for polymer−polymer termination rates,[18−21] whose main results can be summarized as

$$k(N, M \gg N) \rightarrow k(N), \quad k(N) \sim \frac{1}{N^{\alpha}} \begin{cases} \alpha < 1 & (N < N_e) \\ \alpha = {}^3/_2 & (N > N_e) \end{cases} \tag{1}$$

where $k(N,M)$ is the termination rate constant between two living polymers with degrees of polymerization N and M. The first relation is the "small wins" principle: the short chain dominates[22,23] reaction between two chains of very different length. Here $k(N) \equiv k(N,\infty)$. The second relationship in eq 1 describes different power law decays of k depending on chain length regime. The shortest chains have essentially dilute dynamics, and the N dependence is very weak ($\alpha = 0.16$[19]) while somewhat longer chains crossover to unentangled semidilute behavior,[20,21] $\alpha = {}^1/_2$. For longer chains, $N > N_e$, the effects of entanglements begin to dominate and the exponent becomes ${}^3/_2$.[18,20] The crucial feature as far as polymerization rates and MWDs are concerned is that α undergoes a transition from values smaller than unity to values greater than unity, and the chain length N_e is where this crossover occurs.

A technical point is that the scale at which entanglement-dominated kinetics onset is predicted to be larger than N_e for somewhat less reactive radical species (see refs 9 and 20 for details). For clarity's sake, in this paper we take this scale as N_e throughout.

Applying these forms for $k(M,N)$ to the most basic FRP process amounts technically to solving the following dynamics for the living MWD $\psi(N,t)$:

$$\frac{\partial \psi}{\partial t} = -v \frac{\partial \psi}{\partial N} - H\psi, \quad \psi(0,t) = \frac{R_I(t)}{v},$$
$$H(N,t) \equiv \int_0^{\infty} \mathrm{d}M\, k(N,M)\, \psi(M,t) \tag{2}$$

These are FRP kinetics without chain transfer. Here we consider systems (such as PMMA) where transfer is a small enough effect that a typical chain will most likely have terminated before a transfer event can take place (see section V for a discussion). Here the chain propagation velocity is $v \equiv k_p[M]$, where k_p is the propagation rate constant and [M] is monomer concentration. The (generally time-dependent) initiation rate is $R_I(t)$, and $H(N,t)$ is the termination "reaction field" acting on chains of length N due to all other chain lengths M.

These kinetics are nonlinear and nonlocal. In ref 9 they were solved exactly for steady-state FRP (R_I = constant) in the limit of strongly entangled living chains, i.e., the mean living chain length $\bar{N}$ much greater than the threshold for entanglement-dominated kinetics:

$$\bar{N} \gg N_e \tag{3}$$

The meaning of this condition is that most living chains are "long", much longer than N_e. (A typical value[24] of N_e for melts is of the order $N_e \approx 100$, and this might become an order of magnitude greater at, say, 10% conversion. Thus, since N values at higher conversions around 10^4 are common, many FRP systems obey eq 3 at these conversions.) It was shown in ref 9 that the sharp decay of rate constants k for entangled chains ($\alpha > 1$) results in strongly suppressed net long−long termination rates; the dominant termination mechanism is between short chains (length of order N_e) and long chains. The domination of short−long termination was also proposed by other workers.[8,25]

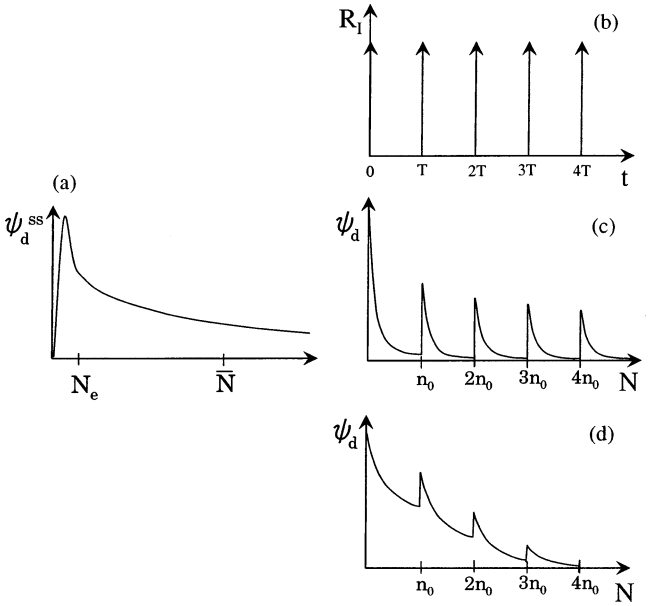

Figure 1. (a). Steady-state dead MWD ψ_d^{ss} predicted by theory of ref 9 for constant rate of initiation, R_I = constant. For most chain lengths, $N > N_e$, the dead MWD is essentially a copy of the living MWD with the same exponential decay and mean living chain length $\bar{N}$. For small N the MWD has linear form. (b) The situation studied in this paper is the polymerization response when the initiation rate is a sequence of pulses spaced by T. (c) Predicted dead MWD for a polymerization initiated by the pulsed initiation sequence of (b) and performed in a background of entangled monodisperse dead chains. The peaks are separated by $n_0 = vT$, the chain length grown between pulses. Most dead chains are concentrated within the entanglement length N_e of the beginning of each cycle. The reason is that the net termination rate of living chains is governed by the rate constant which decays as $k(n) \sim 1/n^{3/2}$ for $n > N_e$, where n is the distance from the beginning of each period. The result is a multimodal form. (d) Comparison with dead MWD after pulsed initiation under *low-conversion* conditions. Peaks are present, but much less pronounced than in (c).

The essential condition for applicability of the present analysis is eq 3. Here we extend the above analysis to the case where R_I is no longer constant, but instead represents a pulse sequence

$$R_I(t) = R_I T \sum_{i=-\infty}^{\infty} \delta(t - iT) \tag{4}$$

as illustrated in Figure 1b. Before detailed calculation, a few rough arguments give insight as to why a multimodal MWD should result from such a pulse sequence. A time τ_{short} ($\equiv N_e/v$) after a new pulse is injected there are no short living chains; i.e., long−long reactions are the only source of termination. But these are very weak due to entanglements. Thus, after τ_{short} termination is virtually switched off, and so most of the dead chain MWD is produced within a time τ_{short} of each pulse. This translates into a multimodal dead MWD (see

Figure 1c) where each peak is broadened by an amount $\approx N_e$. The necessary condition which the delay between pulses T must obey is

$$\tau_{short} < T < \tau_{living}, \quad \tau_{short} \equiv \frac{N_e}{\nu}, \quad \tau_{living} \equiv \frac{\bar{N}}{\nu} \qquad (5)$$

Here τ_{living} is the mean living chain lifetime. In section VI we will estimate time scales for typical systems; for example, we crudely estimate $\tau_{short} \approx 0.04$ s and $\tau_{living} \approx 1.3$ s for PMMA at $\phi = 0.4$, suggesting a pulse period such as $T = 0.2$ s as appropriate.

It follows that by observing the dead MWD in this pulse initiation experiment one can *directly* and quantitatively test the importance of entanglements and the predicted short−long domination. This is the fundamental motivation for our study. Generally, these rather bizarre kinetics are exposed by non-steady-state approaches. For example, switching off radical production at high conversion is predicted[10] to generate living chains which grow for a much longer time than the steady-state lifetime τ_{living}.

Let us briefly compare what is predicted here to what is observed in the widely used low-conversion PLP method.[11−17] In these experiments modulations of the dead MWD are observed.[26−28] These are much less pronounced than those predicted here (compare parts c and d of Figure 1). The essential difference is that there is no short−long domination at low conversion since α is always less than unity. Thus, when T is chosen smaller than τ_{living}, dead chains are generated at similar rates throughout the period between pulses.

Note that the experiment considered here is not a zero conversion PLP experiment continued to high conversion. Since, roughly, $\nu(\phi) \sim k_p^0(1 - \phi)$, it follows that even if k_p^0 is independent of conversion ϕ, the dead MWD peak locations (multiples of νT at any instant) will gradually shift as conversion increases. This loss of coherence will destroy the multimodal features.

The outline of the paper is as follows. In section II we review theory of standard steady-state high-conversion FRP, driven by constant initiation. The concept of short−long domination emerges, and the steady-state living and dead MWDs will turn out to be closely related to those produced in the non-steady-state situation. In section III we turn to non-steady-state FRP driven by a pulsed initiation sequence. The domination of short−long termination events is again critical in determining the living MWD. In section IV the dead MWD is determined from the living MWD. We show it consists of a sequence of peaks of width of order N_e. Section V addresses the extension of the method to nonmonodisperse dead chain backgrounds, such as the broad dead MWD produced by a standard steady-state FRP. We show multimodality survives, provided certain conditions apply. The robustness with respect to other potential problems such as propagation rate changes with conversion, and chain transfer is also discussed. In section VI we conclude with a brief discussion, and we quantitatively estimate dead MWDs we would expect in typical real pulse-driven experimental high-conversion polymerizing systems.

II. Review of Steady-State FRP: Short−Long Termination

As preparation for the more complex pulsed FRP, in this section we first review the closely related high-conversion FRP at steady state, as analyzed theoretically in ref 9. The dead chain matrix is assumed above the entanglement threshold; i.e., sufficiently long living chains are entangled.

The living MWD is now the steady-state solution of eq 2 with constant initiation rate, $R_I(t) \rightarrow R_I$. If we can deduce the reaction field $H(N)$, this will give us the living MWD according to

$$\psi(N) = \psi(0) e^{-\int_0^N dN' H(N')/\nu} \qquad (6)$$

The reaction field has rather simple forms for large and for small N. Now for small N, most chains M contributing to the net reaction field are much bigger than N, i.e., $k(N,M) \approx k(N)$ (the "small wins" principle). Thus

$$H(N \ll n^*) = k(N)\psi_l, \quad \psi_l \equiv \int_0^\infty dN\, \psi(N) \qquad (7)$$

where ψ_l is the total number of living chains. The scale n^* will be discussed below.

Meanwhile for large enough N the dominant M values are smaller than N and $k(N,M) \approx k(M)$ so the field on long chains is actually independent of chain length

$$H(N \gg n^*) = \int_0^\infty dM\, k(M)\, \psi(M) \equiv H_s \qquad (8)$$

Now we can estimate the magnitudes of the short and long chain forms as

$$H(N \ll n^*) \approx k(N)\, \psi(0)\bar{N},$$
$$H(N \gg n^*) \approx N_e k(N_e)\psi(0) \qquad (9)$$

These are not precise expressions but rather estimates understood to be accurate only to within prefactors of order unity. To obtain the long-chain form, we used the fact that the total number of chains equals the MWD width $\bar{N}$ times a characteristic MWD amplitude taken as its value at the origin. The estimate of the short-dominated field acting on long chains, H_s of eq 8, is of the displayed form because the integral defining it is dominated by chain lengths of order N_e. This is a crucial point. It hinges on (i) the small wins principle and (ii) the reaction exponent α being greater than unity for $N > N_e$ and less than unity for $N < N_e$ (see eq 1). Since $\psi(M)$ is much broader ($\bar{N} \gg N_e$), it is a slowly varying function multiplying $k(M)$ and the domination of $M \approx N_e$ follows.

Using these estimates, we can also estimate the crossover scale n^* at which short- and long-chain forms of the reaction field are equal

$$n^* \approx N_e \left(\frac{\bar{N}}{N_e}\right)^{2/3} \qquad (10)$$

The physical interpretation of these results is that *almost all terminations are short−long events*. That is, short chains ($N < n^*$) almost certainly terminate with a member of the majority long chain group, whose typical length is the mean length $\bar{N}$. This was reflected by the reaction field on short chains being dominated by the total number, ψ_l. On the other hand, a long entangled chain almost certainly terminates with a short unentangled chain of length N_e or less. This is a direct result of the powerful suppression of chain mobility due to entanglements. A given long chain is

much more likely to react with a mobile small chain: although there are many more long entangled chains, their diffusivities are so suppressed that their net contribution is small. This was reflected by the reaction field on long chains, H_s, being dominated by unentangled chains of length N_e or less.

Short−long domination has various interesting and simplifying consequences. Consider a living chain which has just been initiated ($N = 0$) and starts to grow. This chain will eventually terminate either as a short chain or as a long chain. Suppose the probabilities of these two outcomes are x and y. Now since we know the total rate at which short chains terminate equals that for long chains (all terminations involving a short−long pair), it follows that $x = y = {}^1/_2$. Hence, the probability the chain survives to grow to length n^* (the short−long field dividing point) must equal ${}^1/_2$ exactly, and it follows that $\psi(n^*) = \psi(0)/2$ (see ref 9 for a more detailed explanation).

We can now deduce the living MWD:

$$\psi(N < N_e) = \psi(0)e^{-c(N/N_e)^{(1-\alpha)}},$$
$$\psi(N \gg N_e) = \frac{\psi(0)}{2}e^{-N/\bar{N}}, \quad \bar{N} \equiv \frac{v^2 2 \ln 2}{R_I \int_0^\infty k} \tag{11}$$

where c is a constant. The derivation of $\bar{N}$ is presented in Appendix A.

The final product of FRP is the dead MWD. The instantaneous dead MWD (the rate dead chains of length N are being produced) is

$$\dot{\psi}_d(N) = \int_0^{N/2} dM\, k(N - M, M)\, \psi(N - M)\, \psi(M) \tag{12}$$

For long entangled chains, $N > N_e$, the integration is dominated by $M \approx N_e$ since the rate constant k falls of sharply with the ${}^3/_2$ entangled power law for larger M. Using the small wins principle once again, one obtains

$$\dot{\psi}_d(N) = H_s \psi(N) \qquad (N \gg N_e) \tag{13}$$

Thus, for longer chains the dead MWD is simply a copy of the living. By contrast, for a given short dead chain length ($N \ll N_e$) all living chains with lengths between 0 and N contribute significantly. The living MWD is practically constant in this range ($\psi(M) \approx \psi(0)$). Thus

$$\dot{\psi}_d(N) \approx \frac{\psi(0)^2}{2} N k(N) \qquad (N \ll N_e) \tag{14}$$

Because $\alpha < 1$ near the origin, $\psi_d(N) \sim N^{1-\alpha}$ vanishes at $N = 0$ (while the living MWD diverges). The predicted steady-state dead MWD is sketched in Figure 1a.

III. Laser Pulsed FRP: Living MWD

We now consider FRP in the same entangling background matrix as in section II, but now the polymerization is driven by the pulse initiation rate sequence $R_I(t)$ of eq 4. We begin in this section with the living MWD.

Since the pulse sequence is periodic with period T, the FRP will settle down to a stationary state with the same period:

$$\psi(N, t) = \psi(N, t + T), \quad H(N, t) = H(N, t + T) \tag{15}$$

In all following discussions, "time" t will be measured relative to the beginning of a period, $0 \le t < T$.

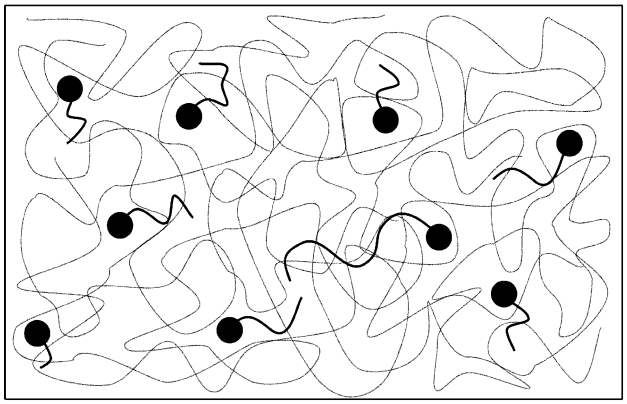

Figure 2. Schematic of living chains with live radical ends, growing and terminating in a matrix of monodisperse inert chains plus unpolymerized monomer solvent. The matrix chains are long enough and concentrated enough to be entangled, such that living chains longer than N_e are also entangled. This strongly suppresses living chain termination rates.

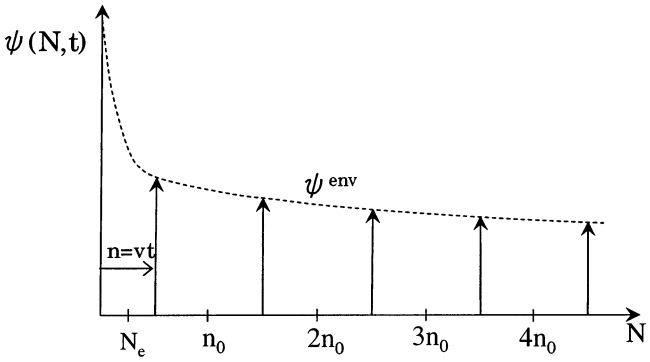

Figure 3. The living MWD is a sum of delta pulses separated by n_0. Their envelope, which the pulse amplitudes follow smoothly, is the living MWD envelope, $\psi^{env}(N)$. Pulses move with velocity v. The quantity n is defined to be the length of chains belonging to the youngest pulse, $n = vt$ where $0 \le t < T$.

At the beginning of each period, $R_I T$ new living polymers ($N = 0$) are introduced per unit volume. These grow to length

$$n_0 \equiv vT \tag{16}$$

until the next pulse arrives. Thus, the living MWD $\psi(N,t)$ is a sum of delta pulses, separated by n_0, traveling with velocity v along the N-axis (see Figure 3). At any instant the shortest chain has length vt (recall that t is always measured relative to the time of injection of the last pulse, $0 \le t < T$). Let us define the envelope of these pulses, $\psi^{env}(N)$, so that

$$\psi(N, t) = \psi^{env}(N) n_0 \sum_{i=0}^{\infty} \delta(N - (in_0 + vt)) \tag{17}$$

With this definition, after time-integrating eq 17 over one period and using eq 4, it follows that the boundary condition is the natural generalization of that in steady state, $\psi^{env}(0) = R_I/v$.

Before proceeding, let us define an important quantity. We will associate with every chain length N a quantity n, namely the *remainder* of N modulo n_0. Thus

$$N = in_0 + n \tag{18}$$

where i is an integer. Throughout, we will find this quantity $0 \le n < n_0$ is an important characteristic, telling us where N lies in the interval it belongs to between in_0 and $(i + 1)n_0$.

To obtain the envelope MWD, we substitute eq 17 into the living dynamics eq 2, yielding

$$\left[v \frac{\partial \psi^{\mathrm{env}}(N)}{\partial N} + H(N, t)\psi^{\mathrm{env}}(N) \right] \times \sum_{i=0}^{\infty} n_0 \delta(N - (in_0 + vt)) = 0 \quad (19)$$

where the time independence of ψ^{env} was used, and the reaction field is obtained from the general definition (eq 2) using the stationary living MWD of eq 17. Consider a fixed value of N. Now since this equation must be true for all t, the expression in the square brackets must vanish when the argument of the delta function vanishes, i.e., when $vt = n$. At this moment the reaction field has strength

$$H^{\mathrm{env}}(N) \equiv H(N, n/v) = n_0 \sum_{i=0}^{\infty} k(N, in_0 + n)\, \psi^{\mathrm{env}}(in_0 + n) \quad (20)$$

H^{env} is the relevant reaction field in stationary state. Its form reflects the fact that there is just one moment in the period $0 \le t < T$ when chains of length N are present in the living MWD. At this moment, $t = n/v$, this chain feels a reaction field due to all those chains of lengths $N \pm jn_0$ which are simultaneously present at that instant. Thus, we have

$$v \frac{\partial \psi^{\mathrm{env}}(N)}{\partial N} = -H^{\mathrm{env}}(N)\, \psi^{\mathrm{env}}(N) \quad (21)$$

We recover the steady-state equation, but now for the envelope function.

Similarly to steady state, the reaction field $H^{\mathrm{env}}(N)$ has simple limiting forms for short and long chains. We find these limiting forms are very similar to those of steady state (see eqs 7 and 8) and are given by

$$H^{\mathrm{env}}(N \ll n^*) = k(N)\psi_l{}^{\mathrm{env}},$$
$$H^{\mathrm{env}}(N \gg n^*) = H_s{}^{\mathrm{env}}(N) \equiv n_0\, k(n)\psi^{\mathrm{env}}(n) \quad (22)$$

Here $H_s{}^{\mathrm{env}}$ is the reaction field acting on long chains, the counterpart of H_s in steady state (see eq 8). Like steady state, the dominant contribution comes from short chains. However, a big difference is that it depends on N. The results of eq 22 are derived in Appendix C, where error terms are evaluated, and it is shown the crossover n^* is unchanged from steady state. These fields are sketched in Figure 4.

Two comments are necessary. (1) The short chain form is dominated by long chains and is proportional to the number of living chains whose relative number changes during each cycle by only a small amount $\epsilon \approx n_0/\bar{N} \ll 1$. Thus, it can be replaced with its time average, $\bar{\psi}_l$. But this time average is exactly equal to the area under the living MWD envelope, $\psi_l{}^{\mathrm{env}} \equiv \int_0^\infty \psi^{\mathrm{env}}(N)$. See Appendix B for detailed explanation. (2) The long-chain form $H^{\mathrm{env}}(N)$ is *dominated by the youngest pulse*, $i = 0$. This pulse is especially powerful, its strength diverging

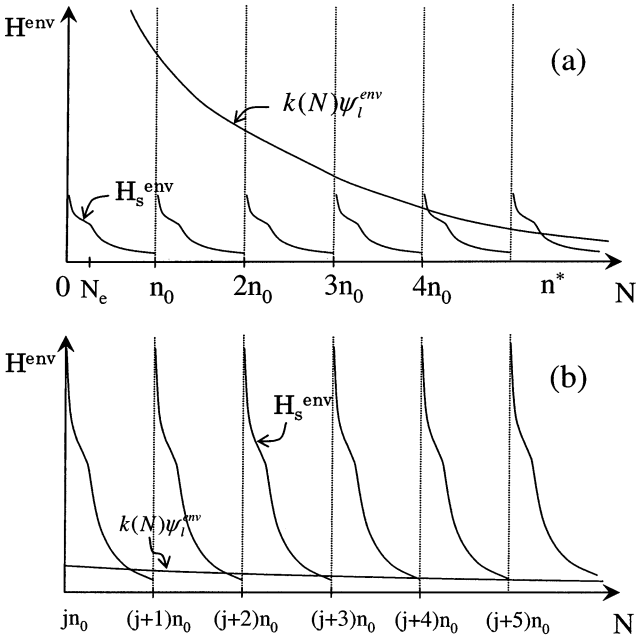

Figure 4. Reaction fields for small and large N. (a) The dominant reaction field on short chains is $k(N)\psi_l{}^{\mathrm{env}}$. Also plotted is $H_s{}^{\mathrm{env}}$ (the field which dominates for large N) which in this domain is much smaller than $k(N)\psi_l{}^{\mathrm{env}}$ with the exception of a small interval at the start of each period. The two fields become of comparable magnitude at $N \approx n^*$. (b) For long chains ($jn_0 \gg n^*$) the dominant reaction field is $H_s{}^{\mathrm{env}}$ (for clarity its amplitude is increased relative to (a)). This is essentially the field due to the youngest pulse.

at the beginning of each cycle as $\sim k(n) \sim n^{-\alpha}$. Thus, the net termination rate of a long enough chain of length N is simply its total reaction rate with chains of length n. This has no analogue in steady state and will turn out to be the basic reason the dead MWD has sharp peaks. Unlike steady state, H^{env} depends on chain length.

Note that the statement that the field on short chains is $k(N)\psi_l{}^{\mathrm{env}}$ is actually untrue at the very beginning of each cycle, $0 < t \lesssim \tau_{\mathrm{short}}$, during which period the field from the youngest pulse is stronger. However, as shown in Appendix C, the net effect on the amplitude over one cycle is small. Further, the field on long chains is no longer given by $n_0 k(n)\psi^{\mathrm{env}}(n)$ for times comparable to the period T (then older pulses compete with the youngest). Again (see Appendix D), the net effect on the amplitude over one cycle is small; in fact, virtually all termination for long chains occurs by a time of order τ_{short} during which period the youngest pulse is strongly dominant.

Having the reaction field, the living envelope follows from eq 21:

$$\psi^{\mathrm{env}}(N) = \begin{cases} \psi^{\mathrm{env}}(0) \mathrm{e}^{-\psi_l{}^{\mathrm{env}} \int_0^N k/v} & (N < n^*) \\ (\psi^{\mathrm{env}}(0)/2) \mathrm{e}^{-\bar{H}_s{}^{\mathrm{env}} N/v} & (N > n^*) \end{cases} \quad (23)$$

These results are derived in Appendix E. Note the living MWD long chain form involves the field $\bar{H}_s{}^{\mathrm{env}}$ averaged over a period which is in fact identical to the steady-state long-chain field H_s of eq 8 and determines $\bar{N}$:

$$\bar{H}_s{}^{\mathrm{env}} \equiv \int_0^{n_0} \mathrm{d}n\, H^{\mathrm{env}}(n)/n_0 \approx \int_0^\infty \mathrm{d}N\, k(N)\, \psi^{\mathrm{env}}(N) = v/\bar{N} \quad (24)$$

The living MWD envelope is sketched in Figure 5. For

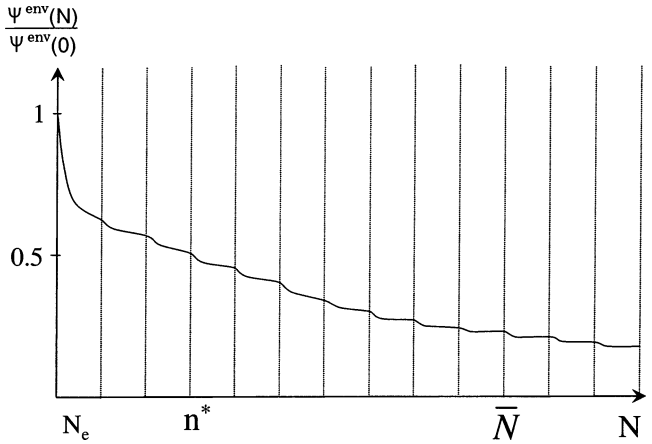

Figure 5. Living MWD envelope ψ^{env} under pulsed initiation in entangled background. The amplitude decays sharply up to order N_e and then decreases more gradually. There is a small step at the beginning of each cycle. For $N > n^*$ this step decrease is the main source of decay, and thus for large N the profile is a gentle staircase.

large N its form is actually a staircase of steps of width n_0, with the step decreases occurring in the first N_e of each cycle (see Appendix D). For the rest of each cycle the steps are rather flat. The exponential form we show above, eq 23, is this staircase coarse-grained over scales n_0.

Finally, we remark that we implicitly assumed $n_0 \ll n^*$. We show in Appendix F that in the case where the period n_0 is greater than n^* all of the conclusions above are essentially unchanged, with n_0 now replacing n^* as the dividing line between short and long fields.

IV. Laser Pulsed FRP: Dead MWD

In the previous section we established the living MWD resulting from pulsed FRP in an entangled monodisperse dead chain background. This is very similar to the steady-state analogue. In this section we turn to the dead MWD which is proportional to the time average over one cycle of the rate of generation of chains of length N

$$\bar{\dot{\psi}}_d(N) \equiv \frac{1}{T}\int_0^T dt\ \dot{\psi}_d(N, t) \tag{25}$$

This turns out be completely different than steady state, exhibiting rather sharp multimodal features separated by n_0 (see Figure 1c). The new feature is the domination of termination processes by the *youngest pulse*, those chains most recently injected. These have lengths increasing from 0 to n_0 as time increases from $t = 0$ to $t = T$.

Now we saw that the living MWD comprises discrete delta functions separated by n_0. Consider the instant when the youngest pulse length is n. At this moment the chain lengths that are present in the living MWD are $in_0 + n$. The termination reactions between all possible pairs is thus generating dead chains of lengths $jn_0 + 2n$ (see Figure 6). If we ask when dead chains of some length N are being created, the answer is at two times during each period: at both $t = n/2v$ and $t = (n_0 + n)/2v$. At these times, the living chain lengths whose terminations generate dead chains of length N are pairs

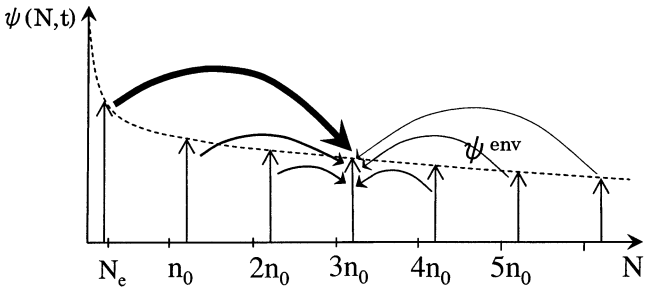

Figure 6. Termination reaction field acting on a given living chain of length $in_0 + n$ is due to all other chains of lengths $i'n_0 + n$. The dominant contribution is from the chains produced by the youngest pulse, and this contribution is substantial only when N_e is of order N_e or less. These terminations produce dead chains of lengths $jn_0 + 2n$.

M_i and $N - M_i$ where

$$M_i = \frac{i}{2}n_0 + \frac{n}{2} \tag{26}$$

and i is an integer between 0 and i_{max} with $N = i_{max}n_0 + n$. Each M_i terminates with $N - M_i$ to give dead chain length N. Adding these discrete contributions to the total dead MWD by substituting eq 17 into eq 12 and time averaging, one obtains

$$\bar{\dot{\psi}}_d(N) = n_0\sum_{i=0}^{i_{max}} k(N - M_i, M_i)\,\psi^{env}(M_i)\,\psi^{env}(N - M_i)$$

$$\approx k(N - n/2, n/2)\psi^{env}(n/2)\psi^{env}(N - n/2) \tag{27}$$

The important step made here is to note that the youngest pulse, $M_0 = n/2$, provides the dominant contribution to $\bar{\dot{\psi}}_d$. This is essentially because rate constants fall off as $k(N) \sim N^{-3/2}$ for $N > N_e$, and hence most termination is due to N values of order N_e (occurs for times of order τ_{short} near the beginning of each cycle). Since older pulses contain chains longer than n_0, their effect is much weaker than the youngest pulse. Their small relative contribution is calculated in Appendix G.

There are now two cases to consider. (i) For $N > n_0$ we can replace $k(N - n/2, n/2) \approx k(n/2)$ since the only important values of n are order N_e, and for these values $N - n/2$ is much greater than $n/2$ so the "small wins" principle is applicable. Similarly, in the arguments of the envelope living MWD ψ^{env} we can set $n = 0$ with little error. This gives

$$\bar{\dot{\psi}}_d(N) \approx n_0 k(n/2)\psi^{env}(n/2)\psi^{env}(N)$$
$$= H_s^{env}(n/2)\psi^{env}(N) \qquad (N > n_0) \tag{28}$$

where H_s^{env} is the reaction field acting on long chains, $H_s^{env}(N) \equiv n_0 k(n)\psi^{env}(n)$ (see eq 22). (ii) For dead chain lengths in the first sector $N < n_0$ the only possible source is termination between two living chains belonging to the youngest pulse, i.e., of lengths $n/2$. Note that in this sector one has $N = n$. Thus, one has exactly

$$\bar{\dot{\psi}}_d(N) = n_0 k(N/2, N/2)(\psi^{env}(N/2))^2$$
$$\approx H_s^{env}(N/2)\psi^{env}(N/2) \qquad (N < n_0) \tag{29}$$

Note the equal length rate constant $k(N/2, N/2)$ scales identically to $k(N/2)$ differing only by a prefactor.

Equations 28 and 29 are the two main results of this paper. Since ψ^{env} is a slowly varying function, the dead MWD profile is dominated by the rate constant dependence, $k(n) \sim 1/n^{3/2}$ for n bigger than N_e. This is a fast decay and means most of the normalization is contained in chain length values up to order several N_e. No matter what sector N belongs to, the dead MWD decays as $1/n^{3/2}$ in that sector. This is a multimodal distribution which is sketched in Figure 1c.

V. Practical Issues as a Method To Generate Multimodal MWDs

Our aim in this study has been to elucidate the basic principles underlying a method to generate multimodal MWDs by laser pulsing. So far this paper has analyzed the simplest, best-defined situation imaginable which can achieve this: a monodisperse background of long dead chains. In this section we discuss the robustness of the method, beginning with situations where the background matrix is broad and relatively ill-defined. We show that mulitmodality still results, provided certain conditions are obeyed.

Broadly Distributed Dead Chain Backgrounds. Preparing a monodisperse background is tedious and probably not commercially viable. A simpler procedure is to run a steady-state FRP up to a conversion which is high enough that the mean length of the dead chain background, $\bar{N}_{back}$, exceeds N_e. This might be thermally initiated or photoinitiated. At this point pulsing begins. Then none of the conclusions we have reached are altered: even though the dead background now follows a broad MWD (of exponential form for large N, according to theory[9]) the key property is that a substantial fraction of the dead background is above N_e such that long living chain dynamics are strongly entangled. Thus, a multimodal MWD still results.

A major new issue, however, is distinguishing the multimodal MWD due to the pulsing episode from the broad background MWD at volume fraction ϕ, say. (Note that when the background was monodisperse this was not an issue because its chains were all of different lengths to those produced by pulsing, so GPC equipment can readily distinguish.) Consider a peak of width $\approx N_e$ belonging to the multimodal MWD $\dot{\psi}_d(N)$ (see Figure 1c). Now a fraction $N_e/\bar{N}_{back}$ of the broad background dead chains have lengths in the region on the N-axis occupied by this peak. The amount of such background chains is hence proportional to $\phi N_e/\bar{N}_{back}$. On the other hand, the number of multimodal chains is proportional to $\delta\phi n_0/N$, where $\bar{N}$ is the mean dead multimodal chain length and we suppose the pulse episode is continued until the conversion increases from ϕ to $\phi + \delta\phi$. Thus, for the multimodal MWD to be readily distinguishable from the background requires the increment in conversion to obey

$$\frac{\delta\phi}{\phi} \gtrsim \frac{N_e}{n_0}\frac{\bar{N}}{\bar{N}_{back}} \tag{30}$$

In other words, enough pulse-generated chains must be created to distinguish them from the background. The larger the interval between pulses and the larger the background mean chain length, the easier it is to satisfy this condition.

Note that an advantage of this broad background method is that there is no induction period for the FRP to worry about. When a monodisperse background is used, since a typical FRP may need an induction period lasting minutes[29] to settle down to steady state (during which period radicals consume various impurities such as oxygen) the very earliest phase of the pulsing will probably generate an inferior MWD. Pulsing must then be continued beyond this point. If instead a steady-state FRP is run to high conversion before pulsing, the induction episode occurs during the steady-state phase.

Constancy of Propagation Rates. Multimodality relies on coherence of chain growth as conversion increases during the pulsing episode. That is, the chain propagation velocity v must be approximately constant as the pulsing proceeds. In fact, as conversion increases one expects v to decrease since $v(\phi) \sim k_p^0(1 - \phi)$ whence $(\delta v/v) \sim -\delta\phi/(1 - \phi)$ (assuming constant k_p^0). The resultant shift in peak position must be smaller than the peak width N_e if this effect is unimportant. Hence, for the first peak or two (at $N = n_0$ and $N = 2n_0$) to remain coherent we must have $|\delta(vT)| \lesssim N_e$, or

$$\delta\phi \lesssim (1 - \phi)\frac{N_e}{n_0} \tag{31}$$

Thus, the increase in conversion during pulsing, $\delta\phi$, must not be too large. The condition for the jth peak to remain sharp is stricter, $\delta\phi \lesssim (1 - \phi)N_e/jn_0$.

The two conditions (30) and (31) imply that if the method is to be successful in a broad background matrix, then the conversion increase $\delta\phi$ must lie in a certain window. The smaller ϕ, the larger this window.

If one looks ahead at possible commercial application, a realistic system might involve quasi-statically increasing the pulse separation T as conversion increases, in such a way as to precisely negate the shift of the peaks due to the reduction of v with increasing conversion.

Chain Transfer. Real growing living polymers transfer their radicals to the environment at a certain species-dependent rate.[1] Provided this rate is small enough, our conclusions are unaffected: the condition to be satisfied is $\bar{N} < \bar{N}_{tr}$ where $\bar{N}_{tr} \equiv 1/C_{tr}$ is the inverse of C_{tr} the chain transfer coefficient[1] and $\bar{N}$ is the living mean chain length neglecting chain transfer, as calculated in this paper. The meaning of $\bar{N}_{tr}$ is the mean length a living chain grows to before one transfer event occurs. If this is large compared to $\bar{N}$, then most chains have anyway terminated before transfer can interfere and provide a substantial incoherent background superposed on the multimodal MWD.

In the case of PMMA, for example, we have[30] $C_{tr} \approx 8 \times 10^{-6}$ so $\bar{N}_{tr} \approx 1.25 \times 10^5$ is almost always much larger than $\bar{N}$ for which typical values[6] are less than 10^4. Another example is poly(vinyl acetate), for which[30] $C_{tr} \approx 2 \times 10^{-4}$ and $\bar{N}_{tr} \approx 5000$. Again this is much larger than the entanglement length and usually larger than or of order $\bar{N}$. For these two species, then, chain transfer is not expected to interfere with the multimodal result. However, polymer species with much larger transfer rates will not be amenable to our approach.

How Universal Are Our Findings? Our results hinge on certain properties of the termination rate constants, $k(M,N)$, as summarized in eq 1. In the literature, various other forms for $k(M,N)$ have been quoted. However, it is important to appreciate that there is something very special about the form shown in eq 1: if one assumes that the polymers are well-behaved coils following the static and dynamic laws[31,32] established by a vast body of research for polymer solutions

and melts across many species, then these forms are universally valid and no "alternative" form for $k(M,N)$ is acceptable. This has been established by a series of first principles theoretical works.[33] On the other hand, it may be that complex effects (such as association, glassiness, side reactions, etc.) lead to some effective rate constants which have different forms embodying these effects. Even then, the "small wins" principle (the first requirement in eq 1) is quite general and always valid. The second requirement can in fact be weakened to $\alpha < 1$ and $\alpha > 1$ for respectively $N < z$ and $N > z$. That is, there must exist some scale z separating two different behaviors for k, a decay slower than $1/N$ and a decay faster than $1/N$. These are rather broader conditions.

Nonuniformity of Irradiation. Laser irradiation normally produces spatially varying intensities across the FRP sample. This means the initiation rate due to pulsing, $R_I(t)$, depends also on position in the sample. The result is a superposition of multimodal MWDs each of the form depicted in Figure 1c, but each with a different mean initiation rate R_I. Since these all have the same spacing between peaks, n_0, and the same peak widths N_e, this will not affect coherence of the multimodal product. The net amplitude of each peak will be a spatial average of the position-dependent amplitude. In summary, nonuniformity of irradiation does not upset multimodality.

Note also that none of our conclusions are affected by the fact that each initiation event results in a pair of nearby radicals, since correlations between two such radicals are lost in a microscopic time scale of order the single molecule diffusion time. (This is because small molecules explore space noncompactly in three dimensions.[18]) In the time scale for one monomer to be added to the growing chains (typically $\sim 10^{-3}$ or 10^{-4} s) the two freshly created polymers are able to diffuse far apart from one another (except for the very highest conversions.) Thus, in effect, new living chains are created at random positions in the sample. For these reasons, this is a standard assumption in FRP modeling work.[9]

VI. Discussion

This paper has examined pulsed free radical polymerization (FRP) in a matrix of long entangled inert chains plus monomer solvent. Our main prediction is that the dead MWD is multimodal; in other words, this approach can manipulate the MWDs produced by FRP which is normally associated with broad featureless profiles. One could imagine other novel environments such as gels, with fixed mesh size, whose entangling effect would also produce multimodal MWDs.

While we have focused on a very well-defined situation, we expect similar phenomena to occur when the background is not monodisperse but has nonetheless a significant fraction of long entangled chains as is produced by standard continuously initiated FRP carried up to high conversion. We discussed certain restrictions on the increment in conversion, $\delta\phi$, during the pulsing. This must be small enough that propagation rates do not change substantially, while it must be large enough to distinguish the multimodal product from the background.

The essential origin of these effects is short−long domination of termination processes when entanglements are present. Theory of steady-state FRP has predicted[9] most terminations involve reaction between a short *mobile* living chain and a long *immobile* long chain *provided* two conditions hold: (i) the short chain length dominates the rate constant for termination between a short−long pair, and (ii) for long chains the termination rate decays faster than $1/N$, $k(N) \sim 1/N^{\alpha}$ with $\alpha > 1$. (We refer the reader to ref 9 for discussions of these issues.) Condition ii is only satisfied when living chain center of gravity diffusion is drastically slowed down by entanglements; then theory[18,20] predicts $\alpha = {}^3/_2$. Hence, "short" and "long" translate to "unentangled" and "entangled", respectively. A slight complexity is that for less reactive radicals the entangled $\alpha = {}^3/_2$ behavior onsets[20] at a scale z somewhat larger than N_e. Qualitatively the conclusions are unchanged, and for simplicity our discussion in this paper has taken the crossover scale as N_e.

If one accepts short−long domination in the steady-state situation, one can easily see the origin of multimodality in the pulsed situation. In steady state short unentangled chains are constantly being injected (at the initiation rate R_I). But in the pulsed situation, a time $\tau_{short} = N_e/v$ after a new pulse is injected all those newly injected living chains have grown to become long, they are all entangled. There are no short chains, and thus termination is switched off. Dead chains are therefore being produced only during the period τ_{short} following each pulse. The dead chains that result from this narrow window of termination activity are due to combinations between the shortest chains (belonging to the youngest pulse) and all other living chains lengths. Since the living chain MWD is a sum of evenly spaced delta functions at any instant, the net result is a multimodal dead MWD with peaks of width of order N_e (see Figure 6).

The experimental testing of our predictions would be interesting not only from a practical viewpoint (testing the feasibility of controlling the FRP product) but also for fundamental reasons. Theoretically, the essence of linear high conversion FRP in its simplest form (uncomplicated by chain transfer effects, etc.) has been predicted to be the domination of termination by short−long events. But this domination is difficult to test in steady state; it is much more naturally probed by *non-steady-state* experiments which interfere with a living chain's transition, during its lifetime, from the short state to the long state. This is predicted to have drastic effects on the MWD.

We predict these effects will occur for period T between pulses satisfying $\tau_{short} < T < \tau_{living}$. Here $\tau_{short} = N_e/v$ is the time for a living chain to grow from birth to become long and entangled, and $\tau_{living} = \bar{N}/v$ is the mean living chain lifetime. As an example, let us estimate what this condition amounts to for PMMA in a 40% polymer volume fraction matrix, $\phi = 0.4$. The entanglement lengths for PMMA can be estimated as $N_e \approx N_e^m/\phi^2 \approx 300$ where $N_e^m \approx 50$ is the conventional entanglement value taken at 170 °C.[5,7,24] Now Sack et al.[6] report instantaneous mean dead chain molecular weights $\bar{N}_d \approx 10^4$ at polymer concentration $\phi = 0.4$ for PMMA initiated by ACN at 0. (Note these are lower temperatures than those for which the above N_e values are reported, so the following estimates are rather crude.) Now the steady-state theory[9] predicts the living and dead mean lengths are approximately equal, $\bar{N} \approx \bar{N}_d$, so we conclude $\bar{N}/N_e \approx 33$ for these PMMA polymerizations. Now according to ref 26 the polymerization velocity for PMMA v at 90 °C approximates 13 000 s^{-1}

at low conversion. If we assume $\nu \sim (1 - \phi)$, then at $\phi = 0.4$ this corresponds to $\nu = 7800\ s^{-1}$. Thus, we estimate $\tau_{short} \approx 0.04$ s and $\tau_{living} \approx 1.3$ s. The pulse period should lie between these two limits. For example, if one choses the pulse period to be 0.2 s (as in typical low conversion pulsed FRP experiments), this corresponds to a chain growth of $n_0 \approx 1600$ between pulses. This should be compared to our predicted dead MWD peak widths $N_e \approx 300$ and the cutoff scale for the dead MWD as a whole, $\bar{N} \approx 10^4$. These are very crude estimates, but they suggest that realistic parameters are able to realize the effects we have studied in this work.

Acknowledgment. This work was supported by the National Science Foundation under Grant DMR 9816374. The authors thank Tom Witten (University of Chicago) for stimulating discussions.

Appendix A. The Mean Living Chain Length $\bar{N}$

In this appendix the relation between $\bar{N}$ and other parameters such as R_I, ν, and $k(N)$ is derived.

Now from the short chain reaction field form (eq 7) we can express the value of the living MWD at the boundary chain length n^* by using eq 6:

$$\psi(n^*) = \psi(0) \exp\left[-\frac{\psi_l}{\nu}\int_0^{n^*} dN\ k(N)\right] \qquad (A1)$$

On the other hand, it was shown in the main text that $\psi(n^*) = \psi(0)/2$. It follows that the total number of living chains can be expressed as

$$\psi_l = \frac{\nu \ln 2}{\int_0^\infty dN\ k(N)} \qquad (A2)$$

where the upper limit of the integral was set to infinity because the integral converges on a scale $N \gtrsim N_e$.

An alternative expression for ψ_l is obtained by integrating the living MWD (eq 11) as

$$\psi_l = \int_0^\infty dN\ \psi(N) = \frac{\psi(0)\bar{N}}{2} \qquad (A3)$$

Here we used the fact that most living chains are long ($\bar{N} \gg n^*$) so integrating the long chain form is sufficient to obtain the total number of living chains.

Comparing the above two expressions for ψ_l, we obtain

$$\bar{N} \equiv \frac{\nu^2 2 \ln 2}{R_I \int_0^\infty k} \qquad (A4)$$

after using the boundary condition $\psi(0) = R_I/\nu$.

Appendix B. Use of the Area under the Envelope Living MWD, ψ_l^{env}, in Short-Chain Reaction Field

We derived the short chain form of the reaction field in eq 22, $H^{env}(N \ll n^*) = k(N)\psi_l^{env}$. In this appendix we justify using ψ_l^{env} in this expression.

Now the true quantity appearing in $H^{env}(N \ll n^*)$ is the time-dependent total number of living chains, $\psi_l(t) = \int_0^\infty dN\ \psi(N,t)$. At the beginning of each period, $R_I T$ new living polymers ($N = 0$) are injected. So the total number of living chains increases by this amount at the beginning of each period

$$\psi_l^{max} - \psi_l^{min} = \psi_l(t \to 0+) - \psi_l(t \to 0-) = R_I T = \psi(0) n_0 \qquad (B1)$$

Now $\psi_l(t)$ always resides between ψ_l^{max} and ψ_l^{min}. Thus, one easily shows that $\psi_l(t)$ is always close to its time average $\bar{\psi}_l$ to within small errors

$$\psi_l(t) = \bar{\psi}_l(1 + O(\psi(0)n_0/\psi_l^{env})) = \bar{\psi}_l\left(1 + O\left(\frac{n_0}{\bar{N}}\right)\right) \qquad (B2)$$

But by double-integrating eq 17 over N and then over t in the range $0 < t < T$, one finds that this time average is exactly equal to the area under the envelope function, $\psi_l^{env} \equiv \int_0^\infty \psi^{env}(N)$. Hence, the time-dependent $\psi_l(t)$ can be replaced with ψ_l^{env} to within small errors.

Appendix C. Short- and Long-Chain Reaction Fields

In this appendix we derive the asymptotic forms of the reaction field for long and short chains as displayed in eq 22. The crossover, n^*, between these two forms is also estimated.

1. Long-Chain Field. The reaction field acting on long chains is dominated by contributions from much shorter chains. Applying the "small wins" principle to the reaction field (eq 20), we have

$$H^{env}(N) \approx n_0 \sum_{i=0}^{\infty} k(in_0 + n)\psi^{env}(in_0 + n) \qquad (C1)$$

Now in the above sum the strongest termination reaction rate contribution is from the very shortest chain ($i = 0$). This is the youngest pulse. The total reaction rate with chains belonging to older pulses ($i \geq 1$) is now separated as follows:

$$H^{env}(N) = n_0 k(n)\psi^{env}(n)\left(1 + \sum_{i=1}^{\infty}\frac{k(in_0 + n)}{k(n)}\right) = n_0 k(n)\psi^{env}(n)\left(1 + g(n/n_0)\left(\frac{n}{n_0}\right)^{3/2}\right) \qquad (C2)$$

where the function $g(x) \equiv \sum_{i=1}^{\infty}(i + x)^{-3/2}$ has a value of order 1 at $0 \leq x \leq 1$. In fact, the error is even smaller when $n < N_e$, where $g(n/n_0)(n/N_e)^{\alpha}(N_e/n_0)^{3/2}$ is the correction term.

This tells us that H^{env} may be approximated by the youngest pulse contribution, $H^{env} \approx H_s^{env}(N) \equiv n_0 k(n) \cdot \psi^{env}(n)$, with relative error of order $(n/n_0)^{3/2}$. This is a small error for n values much less than n_0. Near the end of a period, as n approaches n_0, the relative error become comparable to unity. However, as shown in Appendix D, the effect on the living MWD of the correction terms to H^{env} is very small. Thus, they are irrelevant to this order.

2. Short-Chain Field. The field on short chains is dominated by much longer chains. Again, applying the

small wins principle to the reaction field (eq 20), one has

$$H^{\mathrm{env}}(N) = n_0\sum_{i=0}^{\infty} k(N)\psi^{\mathrm{env}}(in_0 + n)\left(1 + O\left(\frac{N}{\bar{N}}\right)\right) = k(N)\psi_l{}^{\mathrm{env}}\left(1 + O\left(\frac{n^*}{\bar{N}}\right)\right) \quad \text{(C3)}$$

where in the last equation n^* was used as the short−long boundary. This is justified below. Note that we replaced the number of living chains $\psi_l(t) = \sum_{i=0}^{\infty}\psi^{\mathrm{env}}(in_0 + n)$ with its time average $\bar{\psi}_l$ which (see Appendix B) is equal to the area under the living MWD envelope $\psi_l{}^{\mathrm{env}}$.

3. Crossover Scale *n.** The living MWD envelope $\psi^{\mathrm{env}}(N)$ is monotonic decreasing. Its relative decrease over some interval along the N-axis is the exponential of minus the integral of $H^{\mathrm{env}}(N)/v$ over this interval (see eq E1). This is similar to what was described in the steady-state FRP section for the steady-state MWD. Thus, the relative effects of short and long fields over one period of length n_0 is represented by the following ratio

$$\frac{\int_0^{n_0}\mathrm{d}n\ H_s{}^{\mathrm{env}}(N)}{\int_0^{n_0}\mathrm{d}n\ k(N)\psi_l{}^{\mathrm{env}}} = \frac{n_0\int_0^{n_0}\mathrm{d}n\ k(n)\ \psi(n)}{n_0 k(N)\psi_l{}^{\mathrm{env}}} \approx \frac{\psi(0)N_{\mathrm{e}}k(N_{\mathrm{e}})}{\bar{N}\psi(0)\ k(N)} \approx \left(\frac{N}{n^*}\right)^{3/2} \quad \text{(C4)}$$

where $k(N)$ was taken as a constant over a period n_0 which is valid for N values close to n^*. Note in these integrals that N is actually a function of n, $N = in_0 + n$ (see eq 18). From eq C4 we see that the fields become comparable at $N = n^*$. Thus, the short−long boundary is n^*, exactly as it was in steady-state FRP.

4. The Contribution of the Youngest Pulse to the Short-Chain Reaction Field. In the above analysis we estimated that the short-chain reaction field is always $k(N)\psi_l{}^{\mathrm{env}}$. However, even for a short chain there is a small interval of time where in fact the reaction field from the youngest pulse $H_s{}^{\mathrm{env}}$ is dominant. For most of the period this is a negligible correction (eq C4). But $H_s{}^{\mathrm{env}}$ diverges at the beginning of a period since $k(0)$ is infinite; hence, at the beginning of each period $k(N)\psi_l{}^{\mathrm{env}}$ is not the correct expression for the reaction field. It is shown in Appendix D that the effect of the youngest pulse is a small drop in the living MWD with width $\approx N_{\mathrm{e}}$ at the beginning of each period. Its integrated effect over an entire period is shown by eq C4 to be negligible for short chains.

Appendix D. Youngest Pulse Domination at the Beginning of a Period

In this appendix we demonstrate that the effect of the youngest pulse, injected at $t = 0$, lasts a time of order τ_{short} corresponding to a chain length of order N_{e}.

Adopting a similar approach to that used in Appendix C (see eq C4), the net effect of the youngest pulse from a time $t = \lambda N_{\mathrm{e}}/v$ up to the end of the period $t = T$ is measured by

$$\frac{\int_{\lambda N_{\mathrm{e}}}^{n_0}\mathrm{d}n\ H_s{}^{\mathrm{env}}(N)}{\int_0^{n_0}\mathrm{d}n\ H_s{}^{\mathrm{env}}(N)} \approx \frac{\lambda N_{\mathrm{e}}k(\lambda N_{\mathrm{e}})\psi(0)}{N_{\mathrm{e}}k(N_{\mathrm{e}})\psi(0)} = \left(\frac{1}{\lambda}\right)^{1/2} \quad \text{(D1)}$$

Here we compared this net effect to the total effect over a period. Hence, the youngest pulse effect, which is the same thing as the long-chain reaction field $H_s{}^{\mathrm{env}}$, lasts for a period of several N_{e}, after which it decays.

For long chains $H_s{}^{\mathrm{env}}$ is essentially the total reaction field, so the living MWD envelope, which decreases according to the integral of $H_s{}^{\mathrm{env}}/v$ (see eq E1), exhibits a staircase with step decreases in the first few N_{e} of each cycle.

Turning now to short chains, this youngest pulse effect is only a minor correction to the total reaction field. It gives a small "blip" in ψ^{env} at the start of each cycle (see Figure 5).

Note that this analysis shows the effect of H_s itself is important only within a few N_{e} of the beginning of a period. This justifies ignoring the contribution from nonyoungest pulses to the long chain reaction field $H_s{}^{\mathrm{env}}$. This was the error term in eq C2, which became order unity only for n values large compared to N_{e}.

Appendix E. Living MWD of Pulsed FRP

In this appendix the living MWD of eq 23 is derived.

The living MWD envelope function can be deduced directly from the reaction field (eq 21)

$$\psi^{\mathrm{env}}(N) = \psi^{\mathrm{env}}(0)\exp[-\int_0^N \mathrm{d}N'\,H^{\mathrm{env}}(N')/v] \quad \text{(E1)}$$

The short-chain living MWD can be directly evaluated using the short-chain reaction field expression $k(N)\psi_l{}^{\mathrm{env}}$

$$\psi^{\mathrm{env}}(N < n^*) = \psi^{\mathrm{env}}(0)\exp\left[-\frac{\psi_l{}^{\mathrm{env}}}{v}\int_0^N \mathrm{d}N'\,k(N')\right] \quad \text{(E2)}$$

Following the same logic as used for steady-state in section II, exactly half of the chains grow long enough to reach the short−long boundary

$$\psi^{\mathrm{env}}(n^*) = \frac{1}{2}\psi^{\mathrm{env}}(0) \quad \text{(E3)}$$

This enables us to evaluate the living MWD for long chains

$$\psi^{\mathrm{env}}(N > n^*) = \frac{\psi^{\mathrm{env}}(0)}{2}\exp[-\int_{n^*}^N \mathrm{d}N'\,H_s{}^{\mathrm{env}}(N')/v] \simeq \frac{\psi^{\mathrm{env}}(0)}{2}\exp[-\bar{H}_s{}^{\mathrm{env}}(N - n^*)/v] \simeq \frac{\psi^{\mathrm{env}}(0)}{2}\exp(-\bar{H}_s{}^{\mathrm{env}}N/v) \quad \text{(E4)}$$

where the integration of the reaction field $H_s{}^{\mathrm{env}}$ was replaced by its coarse-grained mean value $\bar{H}_s{}^{\mathrm{env}}$. This gives the exponential envelope of the true long-chain

form which exhibits a gentle staircase behavior as described in Appendix D.

Appendix F. The Case of Longer Periods, $n_0 > n^*$

Detailed calculations in the main text focused on the case where $n_0 < n^*$. In this appendix we discuss the case of longer periods, always assuming that $n_0 \ll \bar{N}$, which is the necessary condition to see multimodality in the dead MWD. We find that the results of section III remain essentially unchanged.

In fact, this case is rather simple since newly injected chains experience only one period before they grow to be long chains. In this first period these chains are always the shortest in the living population, even though toward the end of the period they grow to lengths exceeding n^*. Thus, the arguments leading to the short chain form in eq 22 are unchanged, except the boundary is now n_0 rather than n^*:

$$H^{\text{env}}(N < n_0) = k(N)\psi_l^{\text{env}} \tag{F1}$$

On the other hand, chains longer than n_0 are always longer than n^*. So their reaction field is always dominated by the youngest pulse ($i = 0$) as shown in Appendix C (eq C4 remains valid). Hence, the field on long chains is again given by H_s^{env} of eq 22

$$H^{\text{env}}(N > n_0) = H_s^{\text{env}}(N) \tag{F2}$$

Thus, the reaction field asymptotics of eq 22 are recovered, but with the short−long boundary now at n_0 rather than n^*. The living MWD for this case is eq 23 with modified short−long boundary equal to n_0.

Appendix G. Youngest Pulse Domination of Dead MWD

Adopting a similar approach to that used in Appendix C (see eq C2), the strongest dead MWD contribution comes from the reaction in which the youngest pulse ($i = 0$) chains are involved. Let us write the total dead MWD with the older pulses ($i \geq 1$) separated as follows:

$$\bar{\psi}_{\text{d}}(N) \simeq \psi^{\text{env}}(N) n_0 k\left(\frac{n}{2}\right)\psi^{\text{env}}\left(\frac{n}{2}\right)\left(1+\sum_{i=1}^{\infty}\frac{k((i/2)n_0+(n/2))}{k(n/2)}\right)$$

$$= \psi^{\text{env}}(N) n_0 k(n/2)\psi^{\text{env}}(n/2)(1 + g(n/n_0)(n/n_0)^{3/2}) \tag{G1}$$

where the slowly varying function $\psi^{\text{env}}(N - M_i)$ is approximated by $\psi^{\text{env}}(N)$ and the rate constants $k(N - M_i, M_i)$ were replaced by $k(M_i)$; i.e., the smaller of its two arguments was retained which gives the same rate constant to within prefactors of order unity. In fact, the error shown in eq G1 becomes even smaller when $n < 2N_e$, where $g(n/n_0)(n/N_e)^{\alpha}(N_e/n_0)^{3/2}$ is the correction term.

This tells us that the dead MWD may be approximated by $H_s^{\text{env}}(n/2)\psi^{\text{env}}(N)$, essentially counting only the termination that the youngest pulse involved. Near the end of a period, as n approaches n_0, the relative error becomes comparable to unity. However, as shown in Appendix D, the effect of the correction terms on the dead MWD is very small.

References and Notes

(1) Flory, P. *Principles of Polymer Chemistry*; Cornell University Press: Ithaca, NY, 1971.
(2) Norrish, R. G. W.; Smith, R. R. *Nature (London)* **1942**, *150*, 336.
(3) Mita, I.; Horie, K. *J. Macromol. Sci., Rev. Macromol. Chem. Phys.* **1987**, *C27*, 91.
(4) Schulz, G. V.; Husemann, F. *Z. Phys. Chem. B* **1937**, *36*, 183.
(5) Balke, S. T.; Hamielec, A. E. *J. Appl. Polym. Sci.* **1973**, *17*, 905.
(6) Sack, R.; Schulz, G. V.; Meyerhoff, G. *Macromolecules* **1988**, *21*, 3345.
(7) Tulig, T. J.; Tirrell, M. *Macromolecules* **1981**, *14*, 1501.
(8) Russell, G. T.; Gilbert, R. G.; Napper, D. H. *Macromolecules* **1992**, *25*, 2459.
(9) O'Shaughnessy, B.; Yu, J. *Phys. Rev. Lett.* **1994**, *73*, 1723; *Macromolecules* **1994**, *27*, 5067, 5079.
(10) O'Shaughnessy, B.; Yu, J. *Phys. Rev. Lett.* **1998**, *80*, 2957; *Macromolecules* **1998**, *31*, 5240.
(11) Beueremann, S.; Buback, M. *Prog. Polym. Sci.* **2002**, *27*, 191.
(12) Coote, M. L.; Zammit, M. D.; Davis, T. P. *Trends Polym. Sci.* **1996**, *4*, 189.
(13) Olaj, O. F.; Bitai, I.; Hinkelmann, F. *Makromol. Chem.* **1987**, *188*, 1689.
(14) Alexandrov, A. P.; Kitai, V. N. G. M. S.; Smirnova, I. M.; Sokolov, V. V. *Sov. J. Quantum Electron. (Engl. Transl.)* **1977**, *7* (5), 547.
(15) Kornherr, A.; Zifferer, G.; Olaj, O. F. *Macromol. Theory Simul.* **1999**, *8*, 260.
(16) Evseev, A. V.; Nikitin, A. N. *Laser Chem.* **1995**, *16*, 83.
(17) O'Shaughnessy, B.; Vavylonis, D. *Macromol. Theory Simul.* **2003**, *12*, 401.
(18) de Gennes, P. G. *J. Chem. Phys.* **1982**, *76*, 3316−3321, 3322.
(19) Friedman, B.; O'Shaughnessy, B. *Macromolecules* **1993**, *26*, 5726.
(20) O'Shaughnessy, B. *Phys. Rev. Lett.* **1993**, *71*, 3331; *Macromolecules* **1994**, *27*, 3875.
(21) Doi, M. *Chem. Phys.* **1975**, *11*, 107, 115.
(22) O'Shaughnessy, B. *Macromol. Theory Simul.* **1995**, *4*, 481.
(23) Yu, D. H.; Torkelson, J. M. *Macromolecules* **1988**, *21*, 852.
(24) Ferry, J. D. *Viscoelastic Properties of Polymers*, 3rd ed.; John Wiley and Sons: New York, 1980.
(25) Adams, M. E.; Russell, G. T.; Casey, B. S.; Gilbert, G.; Napper, D. H.; Sangster, D. F. *Macromolecules* **1990**, *23*, 4624.
(26) Hutchinson, R. A.; Aronson, M. T.; Richards, J. R. *Macromolecules* **1993**, *26*, 6410.
(27) Hutchinson, R. A.; Paquet, Jr., D. A.; McMinn, J. H.; Fuller, R. E. *Macromolecules* **1995**, *28*, 4023.
(28) Shipp, D. A.; Smith, T. A.; Solomon, D. H.; Moad, G. *Macromol. Rapid Commun.* **1995**, *16*, 837.
(29) Karatekin, E. Dynamics of Free Radical Polymerization. Ph.D. Thesis, Columbia University, New York, 1999.
(30) Hutchinson, R. A.; Richards, J. R.; Aronson, M. T. *Macromolecules* **1994**, *27*, 4530.
(31) de Gennes, P. G. *Scaling Concepts in Polymer Physics*; Cornell University Press: Ithaca, NY, 1985.
(32) Doi, M.; Edwards, S. F. *The Theory of Polymer Dynamics*; Clarendon Press: Oxford, 1986.
(33) Friedman, B.; O'Shaughnessy, B. *Int. J. Mod. Phys. B* **1994**, *8*, 2555.

MA034607M